Imrich Ján (Orcid ID: 0000-0003-1795-951X)

Vilkova Maria (Orcid ID: 0000-0003-2833-7361)

Full NMR assignment of new acridinyl-chalcones, pyrazolino-acridines and spiro[imidazo[1,5-b]pyrazole-4,9'-acridines]

Paulína Slepčíková[1], Ivan Potočňák[2], Tibor Béres[3], Dávid Jáger[4], Ján Imrich[5], Mária Vilková[5]

ORCID

Paulína Slepčíková	0000-0002-9168-3622
Ivan Potočňak	0000-0001-6923-8816
Tibor Béres	0000-0002-5845-6903
Dávid Jáger	0000-0003-1573-1407
Ján Imrich	0000-0003-1795-951X
Mária Vilková	0000-0003-2833-7361

[1]*Department of Organic Chemistry, Institute of Chemistry, Faculty of Science, P. J. Šafárik University, Moyzesova 11, 040 01, Košice, Slovak Republic*

[2]*Department of Inorganic Chemistry, Institute of Chemistry, Faculty of Science, P. J. Šafárik University, Moyzesova 11, 040 01, Košice, Slovak Republic*

[3]*Centre of the Region Haná for Biotechnological and Agricultural Research, Department of the Phytochemistry, Faculty of Science, Palacký University, Šlechtitelů 27, 783 71 Olomouc, Czech Republic*

[4]*Institute of Geotechnics, Slovak Academy of Sciences, Watsonova 45, 040 01 Košice, Slovak Republic*

[5]*Laboratory of NMR, Institute of Chemistry, Faculty of Science, P. J. Šafárik University, Moyzesova 11, 040 01, Košice, Slovak Republic*

Correspondence

Mária Vilková, Institute of Chemistry, Faculty of Science, P. J. Šafárik University, Moyzesova 11, 040 01 Košice, Slovak Republic.

Email: maria.vilkova@upjs.sk

This article has been accepted for publication and undergone full peer review but has not been through the copyediting, typesetting, pagination and proofreading process which may lead to differences between this version and the Version of Record. Please cite this article as doi: 10.1002/mrc.5028

KEYWORDS
Spiro acridine
Pyrazole
Carbothioamide
^{1}H, ^{13}C and ^{15}N NMR studies
Single crystal X-ray crystallography

1 INTRODUCTION

In our continuing search for pharmacologically and structurally interesting acridine derivatives, three new chalcones of acridine **2A–C** have been synthesized and their antiproliferative activity investigated.[1] Among these, (2*E*)-3-(acridin-9'-yl)-1-(2",6"-dimethoxyphenyl)prop-2-en-1-one (**2C**), most effective against human colorectal HCT116 cells (IC_{50} = 4.1 μmol/L), was selected for further studies. Inhibition of cell proliferation was associated with cell cycle arrest in G2/M phase and dysregulation of α, α1 and β5 tubulins. In addition, the compound causes a disruption of the mitochondrial membrane potential and an increase in the number of cells with sub G0/G1 DNA content, which is considered as marker of apoptosis. It also up-regulates proapoptotic expression of Bax, down-regulates anti-apoptotic expression of Bcl-2, Bcl-xL and modulates MAPKs and Akt signalling pathways.[1] In another work [2] we found that **2C** had potent antiproliferative and cytotoxic effects on parental cancer cell lines (PAR, Colo 205) and their resistant sub-lines expressing ABCB1. The combination of **2C** with the anticancer drug doxorubicin led to better inhibition of the both ABCB1 expressing cell lines. These results demonstrated a dual potential of chalcone **2C** to act as a chemotherapeutic as well as a chemosensitizing agent in resistant T-cell lymphoma and colon cancer, with higher sensitivity to cancer cells.[2]

In this study, the chalcones **2A-C** were let to react with hydrazine hydrate to give new 9'-(3-R-4,5-dihydro-1*H*-pyrazol-5-yl)acridines **3A-C.** The **3B,C** pyrazolo-acridines, though prepared, were not used in further syntheses due to low yields and stability at higher temperatures. In contrast to **3B,C**, the pyrazole **3A** reacted with phenyl- and *p*-nitrophenyl isothiocyanate via its 1-NH nitrogen to form 5-(acridin-9'-yl)-*N*-R^1-3-R-4,5-dihydro-1*H*-pyrazole-1-carbothioamide **4Aa** and **4Ab**, respectively. Both these products then spontaneously and rapidly spirocyclized upon standing in DMSO-d_6 to yield new acridine pentacyclic spiro compounds, 5-substituted-2-phenyl-3,3a,5,6-tetrahydro-10'*H*-spiro[acridine-9',4-pyrazolo[1,5-*c*]imidazole]-6-thiones **5Aa** and **5Ab,** resp., in a similar way as we have repeatedly found in the past for various 9-acridinyl derivatives.[3–5]

In the previous studies, [1,2] no NMR data for compounds **2A–C** were presented. Herein, we present the complete NMR data for the derivatives **2A–C**, **3A,B**, **4Aa**, **4Ab** and **5Aa**, **5Ab**, and high-resolution mass spectra (HR-MS) and X-ray analysis for the derivatives **2A** and **4Ab** (Table 1).

2 RESULTS AND DISCUSSION

Acridine-9-carbaldehyde (**1**) was prepared according to a previously published procedure.[6] Base-catalysed reaction of aldehyde **1** with acetophenones in ethanol at room temperature gave chalcones **2A–C** (Scheme 1). Chalcones **2A,B** were refluxed with hydrazine hydrate in ethanol to give pyrazolines **3A,B**. Next, pyrazoline **3A** was treated with phenyl- and 4-nitrophenylisothiocyanate at 80 °C in ethanol. The resulting carbothioamides **4Aa,b** were isolated by filtration of the precipitate formed in the reaction mixture.

^{1}H and ^{13}C NMR chemical shifts of compounds **2A–C** are given in Table 2. The 1D NMR spectra of **2A** (Figures S1 and S2) showed the acridin-9-yl ^{1}H NMR signals at δ_H 8.25 (2H, d, J = 8.7 Hz, H-1',8'), 7.59 (2H, t, J = 7.8 Hz, H-2',7'), 7.83 (2H, t, J = 7.3 Hz, H-3',6'), 8.32 (d, J = 8.8 Hz, H-4',5') (Table 2) and ^{13}C NMR signals at δ_C 125.4 (C-1',8'), 126.7 (C-2',7'), 130.6 (C-3',6'), 130.0 (C-4',5'), 141.2 (C-9'), 124.1 (C-8'a,9'a), 148.4 (C-4'a,10'a) (Table 2). In addition, signals at δ_H 7.59 (1H, d, J = 16.0 Hz, H-2) and 8.68 (1H, d, J = 16.0 Hz, H-3) revealed the presence of a *Z*-chalcone fragment.

The structures of **3A,B** were fully characterized by ^{1}H,^{1}H correlation spectroscopy (COSY, Figures S18 and S24), ^{1}H,^{13}C heteronuclear single-quantum coherence (HSQC, Figures S19 and S25), ^{1}H,^{13}C heteronuclear multiple-bond correlation (HMBC, Figures S20 and S26) and ^{1}H,^{15}N-HMBC (Figures S21 and S27) spectra. The aliphatic region of the ^{1}H NMR spectra (Figures S16 and S22) contain one doublet of doublets of doublets at δ_H 3.36 (1H, ddd, J = 16.8, 13.2, 1.6 Hz for **3A**) and 3.35 (1H, ddd, J = 16.8, 12.8, 1.7 Hz for **3B**) and one doublet of doublet at δ_H 3.85 (1H, dd, J = 16.8, 13.2 Hz for **3A**) and 3.83 (1H, dd, J = 16.8, 12.8 Hz for **3B**) corresponding to H-4a and H-4b, respectively. The remaining signals of the pyrazole spin system appear in the typical aromatic proton frequency range (δ_H 8.00 (1H, dd, J = 5.4, 1.6 Hz, H-1), 6.39 (1H, td, J = 13.0, 5.4 Hz, H-5) for **3A** and δ_H 7.79 (1H, d, J = 5.6 Hz, H-1), 6.34 (1H, td, J = 12.8, 5.6 Hz, H-5) for **3B**) (Table 2 and Figures S16 and S22). HSQC connectivities (Figures S19 and S25) were used to identify protonated carbons and HMBC connectivities (Figures S20 and S26) were used to assign nonprotonated carbons.

1D and 2D NMR spectra of **4Aa** and **4Ab** in DMSO-d_6 and $CDCl_3$ are summarized in Table 3. Both ^{1}H NMR (Figures S64) and ^{13}C NMR (Figures S65) signals of **4Ab** measured immediately after dissolution in DMSO-d_6 were doubled. The same was observed in ^{1}H NMR (Figures S39) and ^{13}C NMR (Figures S40) spectra of **4Aa** upon standing in DMSO-d_6 solution. The doubling of signals demonstrates that pyrazoline-thioamides **4Aa,b** react further in DMSO-d_6 to novel compounds, namely spiro compounds of 9,10-dihydroacridine **5Aa,b** (Scheme 1, Table 4). This spirocyclization proceeded through an intramolecular nucleophilic attack of the thioamidic NH-7 nitrogen of the pyrazoline on the electrophilic C-9' carbon of acridine. The compounds **4A** and **5A** were obtained as an inseparable mixture. No spirocyclization was observed in the $CDCl_3$ solution (Table 3, Figures S33–S38 and Figures S57–S63).

The aliphatic region of the ^{1}H NMR spectrum (Figure S64) of **4Ab/5Ab** in DMSO-d_6 contained pyrazole proton signals at δ_H 3.62 (1H, dd, J = 18.7, 8.3 Hz, H-4a), 4.40 (1H, dd, J = 18.7, 12.8 Hz, H-4b) for **4Ab** and at δ_H 2.37 (1H, dd, J = 18.0, 8.6 Hz, H-4a), 3.37 (1H, dd, J = 18.0, 11.6 Hz, H-4b) and 5.10 (1H, dd, J = 11.6, 8.6 Hz, H-5) for **5Ab**. The H-5 proton signal of **4Ab** derivative also appeared at δ_H 7.34 (1H, dd, J = 12.8, 8.3 Hz). Signals of acridine and a phenyl substituent on C-3 appeared in the aromatic region (Table 3, Figure S64). HSQC connectivities were used to identify the protonated carbons (Figures S69). In particular, Figures S71 and S72 show the unambiguous assignment of the aromatic carbons of acridin-9-yl and phenyl moieties of both derivatives **4Ab** and **5Ab**. Quarternary carbons C-3 (δ_C 156.9), C-6 (δ_C 173.7) and C-9' (δ_C 143.7) of **4Ab** (Figure S74 and S75) and C-3 (δ_C 161.7), C-6 (δ_C 178.7) and C-9' (δ_C 75.6) of **5Ab** (Figure S74 and S75) were assigned by their HMBC connectivity with adjacent protons H-4, H-5 and H-7. Also, the unambiguous assignment of N-1 (δ_N -183.1), N-2 (δ_N -65.9) and N-7 (δ_N -249.0) nitrogen atoms in **4Aa** and N-1 (δ_N -183.7), N-2 (δ_N -59.6) and N-7 (δ_N -220.6) in **5Aa** was made through their observed HMBC connectivities with H-4 and H-5 (Figure S79).

NOESY experiments performed with the **4Ab** derivative allowed the assignment of relative stereochemistry at C-5 carbon. The 2D NOESY spectrum measured in DMSO-d_6 was of little help. In contrast, in the 2D NOESY spectrum measured in $CDCl_3$, a strong correlation was observed between protons H-5 and H-4b, which showed that these protons were in a *syn*-periplanar orientation (the same side of the pyrazole ring). In addition, the weak NOESY correlation observed between H-5 and H-4a indicated that these protons were in an *anti*clinal orientation (opposite side of the pyrazole ring, Figure S60). The results were supported by

a coupling constant $^3J_{H5H4b}$ = 12.8 Hz (indicating the *syn*-periplanar orientation) and a value of $^3J_{H5H4a}$ = 8.7 Hz (indicating an *anti*clinal orientation, Table 3). The findings are consistent with the X-ray analysis (Figure 4).

The structures of derivatives **2A** and **4Ab** were confirmed by X-ray analysis. Molecular structures of **2A** and **4Ab** are shown in Figure 4, while crystal data and structure refinement appear in Table 5. As expected, all aromatic moieties in both structures are planar. However, the acridine and phenyl ring systems are not coplanar, mainly due to the twisting of the acridine group along the C1–C3 in **2A** and C3–C5 bond in **4Ab**. The twist is apparently caused by intermolecular hydrogen bonds; C2—H2···N10^{i} (i = 1 – *x*, 2 – *y*, 1 – *z*) in **2A**, and C4—H4B···N10^{i} (i = 2 – *x*, 1 – *y*, 2 – *z*) in **4Ab** (Table S9), joining two inversely related molecules of the title compounds into dimers (Figures S80 and S81). Obviously, the hydrogen bonds in **4Ab** play a vital role in the arrangement of the molecule. Due to the intramolecular N7—H7···N2 and C2'''—H2'''···S8 hydrogen bonds (Table S9), the nitrophenyl, pyrazole and phenyl rings are almost coplanar. Moreover, intermolecular hydrogen bonds assemble the **4Ab** molecules to a final supramolecular arrangement (see below).

The search for π-π interactions in **2A** and **4Ab** has shown that above formed dimer in **2A** is further stabilized by a pair of centrosymmetrically related π-π interactions between aromatic rings with Cg1 and Cg2^{i} centroids (Figure S80). The dimer in **4Ab** is supported by π-π interaction between rings with Cg1 and Cg1^{i} centroids and two pairs of centrosymmetrically related π-π interactions between rings with Cg1 and Cg2^{i}, and Cg2 and Cg3^{i} centroids (Figure S81). Finally, the dimers are arranged in *zig-zag* layers due to the intermolecular C5'''—H5'''···O8'''^{iii} (iii = 1 – *x*, ½ + *y*, ½ – *z*) hydrogen bond system (Table S9). The crystal structure is stabilized by nonspecific interactions between these layers.

3 EXPERIMENTAL

Analytical TLC was performed on pre-coated aluminium plates of silica gel 60 F254 (Merck, Germany), and the compounds were visualized in the UV light. The melting points were recorded on a Boetius instrument and are uncorrected. Nuclear magnetic resonance data were collected on a Varian VNMRS 600 MHz spectrometer operating at 599.87 MHz for ^{1}H, 150.84 MHz for ^{13}C, and 60.79 MHz for ^{15}N. The concentration of all samples was approximately 10 mg/0.6 mL of DMSO-d_6 (chemical shifts were referenced to residual solvent peak: ^{1}H NMR 2.50 ppm and ^{13}C NMR 39.5 ppm) or $CDCl_3$ (chemical shifts were referenced

to TMS 0.0 ppm). NMR data were recorded at 300 K, with chemical shifts δ reported in parts per million and coupling constants *J* in Hertz. The ^{15}N chemical shifts were obtained from two dimensional ^{1}H,^{15}N-HMBC experiments with gradient coherence selection, performed using a standard pulse sequence from the Varian pulse library. For the ^{15}N chemical shifts, CH_3NO_2 was used as an external reference (0.0 ppm). 2D NMR experiments gCOSY, zTOCSY, NOESY, gHSQC and gHMBC were performed using the standard Varian software. All data were analyzed using MNova 7.1.1 (2012) software. The spectral acquisition parameters are summarized in Tables S1 and S2.

4 CONCLUSIONS

In conclusion, we have described the full assignment of ^{1}H, ^{13}C and ^{15}N NMR signals as well as the x-ray and HR-MS data of acridine bearing chalcone or pyrazole fragments, including one promising new potential antitumor agent.

ACKNOWLEDGEMENTS

This work was supported by the Grant Agency for Science of the Slovak Ministry of Education (VEGA), a grant. no. 1/0148/19.

REFERENCES

[1] P. Takáč, M. Kello, M. Bago Pilátová, Z. Kudličková, M. Vilková, P. Slepčíková, P. Petik, J. Mojžiš, *Chem. Biol. Interact.* **2018**, *292*, 37–49.

[2] M. Čižmáriková, P. Takáč, G. Spengler, A. Kincses, M. Nové, M. Vilková, J. Mojžiš, *Anticancer Res.* **2019**, *39*, 6499–6505.

[3] M. Vilková, M. Prokaiová, J. Imrich, *Tetrahedron* **2014**, *70*, 944-961 and references cited therein.

[4] D. Sabolová, M. Vilková, J. Imrich, I. Potočňák, *Tetrahedron Lett.* 2016, *57*, 5592-5595.

[5] M. Vilková, M. Šoral, M. Bečka, I. Potočňák, D. Sabolová, T. Béres, M. Dušek, J. Imrich, *Magn. Reson. Chem.* **2019**, *57*, 1–11.

[6] M. Vilková, L. Ungvarská Maľučká, J. Imrich, *Magn. Reson. Chem.* **2016**, *54*, 8–16.

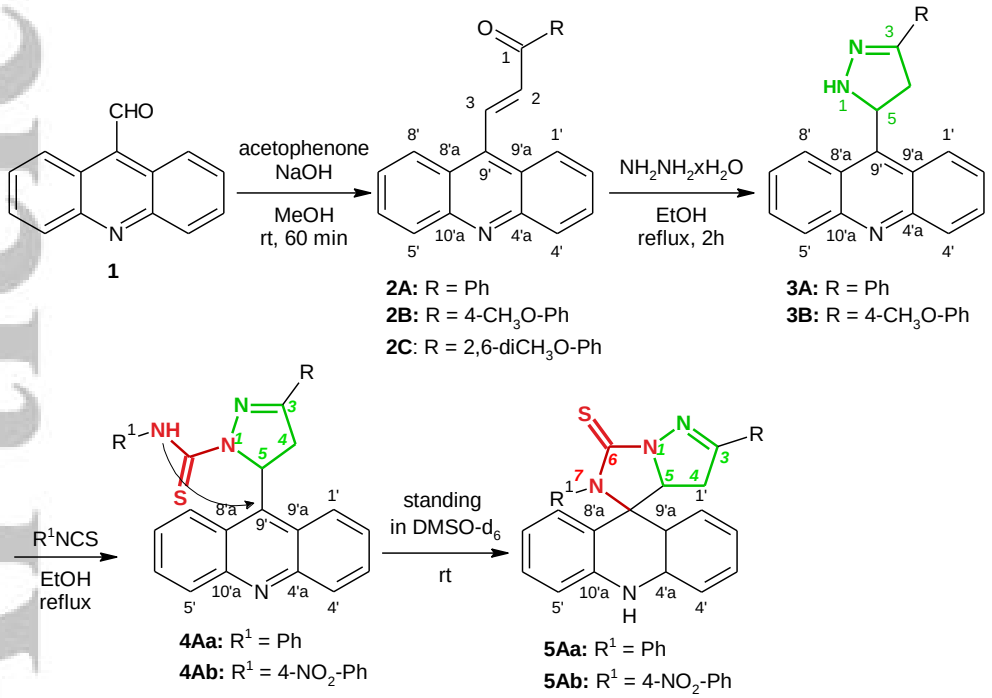

SCHEME 1 Synthesis of 5-(acridin-9'-yl)-*N*-substituted-3-phenyl-4,5-dihydro-1*H*-pyrazole-1-carbothioamides **4Aa,b** and 2-phenyl-5-substituted-3,3a-dihydro-10'*H*-spiro[imidazo[1,5-b]pyrazole-4,9'-acridine]-6(5*H*)-thione **5Aa,b**. The structures are shown along with atom numbering.

TABLE 1 Physico-chemical data for compounds **2A–C**, **3A,B** and **4Aa**,**b**

No.	Name	Melting point [°C]	Yield [mg]	Yield [%]
2A	(2*E*)-3-(acridin-9'-yl)-1-phenylprop-2-en-1-one	148–149	132	88
2B	(2*E*)-3-(acridin-9'-yl)-1-(4"-methoxyphenyl)prop-2-en-1-one	143–144	155	94
2C	(2*E*)-3-(acridin-9'-yl)-1-(2",6"-dimethoxyphenyl)prop-2-en-1-one	177–178	159	89
3A	9'-(3-phenyl-4,5-dihydro-1*H*-pyrazol-5-yl)acridine	208–209	98	93
3B	9'-[3-(4"-methoxyphenyl)-4,5-dihydro-1*H*-pyrazol-5-yl]acridine	200–201	82	79
4Aa	5-(acridin-9'-yl)-*N*,3-diphenyl-4,5-dihydro-1*H*-pyrazole-1-carbothioamide	254–255	52	73
4Ab	5-(acridin-9'-yl)-*N*-(4"-nitrophenyl)-3-phenyl-4,5-dihydro-1*H*-pyrazole-1-carbothioamide	261–262	63	81

TABLE 2 ^{1}H, ^{13}C and ^{15}N NMR data for compounds **2A–C** and **3A,B**[a,b]

No.	2A		2B		2C		3A			3B		
	δ_H (mult., *J*)	δ_C	δ_H (mult., *J*)	δ_C	δ_H (mult., *J*)	δ_C	δ_H (mult., *J*)	δ_C	δ_N	δ_H (mult., *J*)	δ_C	δ_N
1		189.0 (C)		187.1 (C)		193.3 (C-1)	8.00 (dd, 5.4, 1.6)		-235.9	7.79 (d, 5.6)		-237.2
2	7.59(d, 16.0)	133.0 (CH)	7.58 (d, 16.0)	132.7 (CH)	6.95 (d, 16.5)	138.9 (CH)			-40.8			-46.1
3	8.68(d, 16.0)	139.0 (CH)	8.66 (d, 16.0)	138.1 (CH)	8.24 (d, 16.5)	138.4 (CH)		148.4 (C)			148.6 (C)	
4a							3.36 (ddd, 16.8, 13.2, 1.6)	41.3 (CH_2)		3.35 (ddd, 16.8, 12.8, 1.7)	41.7 (CH_2)	
4b							3.85 (dd, 16.8, 13.2)			3.83 (dd, 16.8, 12.8)		
5							6.39 (td, 13.2, 5.4)	57.5 (CH)		6.34 (td, 12.8, 5.6)	57.4 (CH)	
1',8'	8.25 (d, 8.7)	125.4 (CH)	8.25 (d, 8.3)	125.4 (CH)	8.21 (d, 8.3)	125.4 (CH)	8.55 (d, 9.0)	125.0 (CH)		8.56 (d, 8.9)	125.0 (CH)	
2',7'	7.59 (t, 7.8)	126.7 (CH)	7.57 (ddd, 8.7, 6.6, 1.2)	126.4 (CH)	7.56 (ddd, 8.6, 6.5, 1.2)	126.2 (CH)	7.58 (ddd, 9.0, 6.4, 1.4)	125.5 (CH)		7.58 (t, 7.0)	125.5 (CH)	
3',6'	7.83 (t, 7.3)	130.6 (CH)	7.81 (ddd, 8.3, 6.5, 1.4)	130.2 (CH)	7.80 (ddd, 8.7, 6.5, 1.4)	130.1 (CH)	7.83 (ddd, 8.8, 6.4, 1.3)	129.9 (CH)		7.83 (t, 7.0)	129.8 (CH)	
4',5'	8.32 (d, 8.8)	130.0 (CH)	8.27 (d, 8.4)	130.2 (CH)	8.24 (d, 8.6)	130.1 (CH)	8.18 (d, 8.8)	130.1 (CH)		8.17 (d, 8.7)	130.0 (CH)	
9'		141.2 (C)		140.9 (C)		140.4 (C)		145.2 (C)			145.4 (C)	
10'									-74.0			-74.1
8'a,9'a		124.1 (C)		124.0 (C)		123.8 (C)		124.3 (C)			124.3 (C)	
4'a,10'a		148.4 (C)		148.7 (C)		148.6 (C)		148.3 (C)			148.2 (C)	
1''		137.5 (C)		130.4 (C)		117.8 (C)		132.9 (C)			125.6 (C)	
2'',6''	8.10 (d, 6.9)	129.0 (CH)	8.09 (d, 8.8)	131.2 (CH)		158.1 (CH)	7.74 (d, 7.0)	125.7 (CH)		7.67 (d, 8.7)	127.2 (CH)	
3'',5''	7.55 (t, 7.8)	129.1 (CH)	7.01 (d, 8.8)	114.1 (CH)	6.68 (d, 8.4)	104.2 (CH)	7.44 (t, 7.6)	128.6 (CH)		7.00 (d, 8.7)	114.1 (CH)	
4''	7.64 (t, 7.4)	133.7 (CH)		164.0 (C)	7.39 (t, 8.4)	131.7 (C)	7.37 (t, 7.4)	128.3 (CH)			159.6 (C)	
OCH_3			3.90 (s)	55.6 (CH_3)	3.92 (s)	56.1 (OCH_3)					55.2 (O CH_3)	

[a] δ in ppm, *J* in Hz

[b] Compounds were recorded at 600 MHz for ^{1}H, 150 MHz for ^{13}C and 61 MHz for ^{15}N in $CDCl_3$ (**2A–C**) and DMSO-d_6 (**3A,B**).

TABLE 3 ^{1}H, ^{13}C and ^{15}N NMR data for compounds **4Aa** and **4Ab**[a,b]

No.	4Aa (DMSO-d_6)			4Ab (DMSO-d_6)			4Aa ($CDCl_3$)			4Ab ($CDCl_3$)		
	δ_H (mult., *J*)	δ_C	δ_N	δ_H (mult., *J*)	δ_C	δ_N	δ_H (mult., *J*)	δ_C	δ_N	δ_H (mult., *J*)	δ_C	δ_N
1			-187.7			-183.1			-188.2			-184.5
2			-65.0			-65.9			-68.7			-70.8
3		155.7 (C)			156.9 (C)			154.6 (C)			155.8 (C)	
4a **4b**	3.55 (dd, 18.6, 8.4) 4.36 (dd, 18.6, 13.1)	41.5 (CH_2)		3.62 (dd, 18.7, 8.3) 4.40 (dd, 18.7, 12.8)	41.5 (CH_2)		3.52 (dd, 18.0, 8.4) 4.17 (dd, 18.0, 13.2)	42.2 (CH_2)		3.59 (dd, 18.5, 8.7) 4.22 (dd, 18.5, 12.8)	42.3 (CH_2)	
5	7.31 (dd, 13.1, 8.4)	59.6 (CH)		7.34 (dd, 12.8, 8.3)	59.8 (CH)		7.31 (dd, 13.2, 8.4)	59.2 (CH)		7.28 (dd, 12.8, 8.7)	59.2 (CH)	
6		174.4 (C)			173.7 (C)			175.0 (C)			173.3 (C)	
7	10.38 (s)		-250.3	10.77 (s)		-249.0	9.37 (s)		-253.0	9.71 (s)		-251.7
1'	8.73 (d, 9.0)	124.4 (CH)		8.73 (d, 9.0)	124.2 (CH)		8.57 (d, 8.9)	123.4 (CH)		8.56 (d, 8.8)	123.1 (CH)	
2'	7.70 (ddd, 9.0, 6.5, 1.4)	126.2 (CH)		7.73 (ddd, 9.0, 6.5, 1.2)	126.4 (CH)		7.64 (ddd, 8.9, 6.6, 1.3)	126.5 (CH)		7.67 (ddd, 8.9, 6.5, 1.3)	126.7 (CH)	
3'	7.87 (ddd, 8.8, 6.5, 1.2)	129.9 (CH)		7.88 (ddd, 8.7, 6.5, 1.2)	130.0 (CH)		7.80 (ddd, 8.7, 6.5, 1.1)	129.7 (CH)		7.83 (ddd, 8.8, 6.5, 1.1)	129.8 (CH)	
4'	8.18 (d, 8.8)	129.9 (CH)		8.19 (d, 8.7)	130.8 (CH)		8.27 (d, 8.7)	130.7 (CH)		8.29 (d, 8.8)	130.9 (CH)	
5'	8.18 (d, 8.8)	130.7 (CH)		8.19 (d, 8.8)	129.9 (CH)		8.25 (d, 8.5)	131.4 (CH)		8.27 (d, 8.8)	131.6 (CH)	
6'	7.78 (ddd, 8.8, 6.5, 1.3)	129.6 (CH)		7.78 (ddd, 8.8, 6.5, 1.3)	129.7 (CH)		7.70 (ddd, 8.5, 6.5, 1.2)	129.4 (CH)		7.71 (ddd, 8.8, 6.5, 1.2)	129.5 (CH)	
7'	7.51 (ddd, 8.8, 6.5, 1.4)	126.1 (CH)		7.50 (ddd, 9.0, 6.5, 1.4)	126.3 (CH)		7.41 (ddd, 9.0, 6.5, 1.3)	126.5 (CH)		7.41 (ddd, 9.0, 6.5, 1.3)	126.7 (CH)	
8'	7.96 (d, 8.8)	122.9 (CH)		7.92 (d, 9.0)	122.7 (CH)		7.96 (d, 9.0)	122.7 (CH)		7.88 (m)	122.3 (CH)	
9'		144.5 (C)			143.7 (C)			143.1 (C)			142.2 (C)	
10'			-74.3			-73.7			-77.3			-73.7
8'a		122.6 (C)			122.5 (C)			123.1 (C)			122.9 (C)	
9'a		123.9 (C)			124.0 (C)			124.3 (C)			124.3(C)	
4'a		148.1 (C)			148.1 (C)			148.7 (C)			148.7 (C)	
10'a		148.5 (C)			148.5 (C)			149.2 (C)			149.2 (C)	
1''		130.5 (C)			130.2 (C)			130.3 (C)			129.8 (C)	
2'',6''	8.10 (dd, 7.9, 1.8)	127.6 (CH)		8.12 (dd, 8.1, 1.7)	127.7 (CH)		7.86 (dd, 8.1, 1.5)	127.0 (CH)		7.88 (m)	127.2 (CH)	
3'',5''	7.55 (m)	128.8 (CH)		7.57 (m)	128.9 (CH)		7.52 (m)	129.1 (CH)		7.54 (t, 7.5)	129.2 (CH)	
4''	7.55 (m)	131.0 (CH)		7.57 (m)	131.4 (CH)		7.52 (m)	131.3 (CH)		7.57 (t, 7.5)	131.8 (CH)	
1'''	-	139.3 (C)		-	145.7 (C)		-	138.5 (C)		-	144.4 (C)	
2''',6'''	7.45 (dd, 8.4, 1.2)	125.2 (CH)		7.93 (d, 9.3)	123.5 (CH)		7.56 (d, 7.3)	124.0 (CH)		7.91 (d, 9.2)	121.7 (CH)	
3''',5'''	7.28 (t, 7.2)	128.1 (CH)		8.16 (d, 9.3)	123.8 (CH)		7.30 (dd, 8.4, 7.2)	128.6 (CH)		8.16 (d, 9.2)	124.5 (CH)	
4'''	7.11 (dd, 7.2, 1.2)	125.0 (CH)			143.0 (C)		7.14 (t, 7.2)	125.5 (CH)			143.8 (C)	
NO_2						-10.2						-10.2

[a] δ in ppm, *J* in Hz

[b] Compounds were recorded at 600 MHz for ^{1}H, 150 MHz for ^{13}C and 61 MHz for ^{15}N.

TABLE 4 ^{1}H, ^{13}C and ^{15}N NMR data for compounds **5Aa** and **5Ab**[a,b]

No.	5Aa			5Ab		
	δ_H (mult., *J*)	δ_C	δ_N	δ_H (mult., *J*)	δ_C	δ_N
1			-186.8			-183.7
2			-56.6			-59.6
3		160.2 (C)			161.7 (C)	
4a **4b**	2.44 (dd, 18.0, 8.4) 3.33 (dd, 18.0, 12.0)	34.4 (CH_2)		2.37 (dd, 18.0, 8.6) 3.37 (dd, 18.0, 11.6)	34.0 (CH_2)	
5	5.09 (dd, 12.0, 8.4)	73.8 (CH)		5.10 (dd, 11.6, 8.6)	74.0 (CH)	
6		180.1 (C)			178.7 (C)	
7			-219.3			-220.6
1'	7.03 (m)	126.4 (CH)		7.03 (dd, 8.0, 1.3)	125.7 (CH)	
2'	6.85 (ddd, 8.4, 6.6, 1.2)	120.3 (CH)		6.87 (ddd, 8.0, 7.4, 1.2)	120.8 (CH)	
3'	7.28 (ddd, 8.4, 6.6, 1.8)	130.0 (CH)		7.31 (ddd, 8.2, 7.4, 1.2)	130.3 (CH)	
4'	7.03 (m)	115.0 (CH)		7.09 (dd, 8.2, 1.2)	115.2 (CH)	
5'	6.83 (dd, 8.4, 1.2)	114.1 (CH)		6.90 (dd, 8.4, 1.2)	114.3 (CH)	
6'	7.12 (m)	128.9 (CH)		7.15 (ddd, 8.4, 7.2, 1.4)	129.2 (CH)	
7'	6.81 (ddd, 8.4, 6.6, 1.2)	120.1 (CH)		6.78 (ddd, 8.2, 7.2, 1.2)	120.4 (CH)	
8'	7.55 (m)	128.5 (CH)		7.47 (m)	127.9 (CH)	
9'		75.3 (C)			75.6 (C)	
10'	9.55 (s)		-283.4	9.70 (s)		-282.9
8'a		117.0 (C)			116.4 (C)	
9'a		116.3 (C)			115.8 (C)	
4'a		137.5 (C)			137.4 (C)	
10'a		138.3 (C)			138.5 (C)	
1''		130.7 (C)			130.4 (C)	
2'',6''	7.62 (dd, 7.8, 1.2)	126.7 (CH)		7.63 (d, 7.0)	126.9 (CH)	
3'',5''	7.42 (t, 7.8)	128.8 (CH)		7.41 (t, 7.4)	128.8 (CH)	
4''	7.45 (t, 7.8)	130.5 (CH)		7.47 (m)	130.9 (CH)	
1'''		138.5 (C)			144.5 (C)	
2''',6'''	6.98 (dd, 8.6, 1.3)	127.0 (CH)		7.36 (d, 9.2)	126.4 (CH)	
3''',5'''	7.12 (m)	128.1 (CH)		8.03 (d, 9.2)	123.5 (CH)	
4'''	7.03 (m)	126.2 (CH)			144.0 (C)	
NO_2						-10.7

[a] δ in ppm, *J* in Hz

[b] Compounds were recorded at 600 MHz for ^{1}H, 150 MHz for ^{13}C and 61 MHz for ^{15}N in DMSO-d_6.

TABLE 5 Crystal data and structure refinement for **2A** and **4Ab**

Cmpd	2A	4Ab
Empirical formula	$C_{22}H_{15}NO$	$C_{29}H_{21}N_5O_2S$
Formula weight	309.35	503.57
Temperature	173(2) K	173(2) K
Wavelength	0.71073 Å	0.71073 Å
Crystal system	Triclinic	Monoclinic
Space group	*P* 1	$P2_1/c$
Unit cell dimensions	a = 7.2530(3) Å α = 109.889(4)° b = 8.8491(4) Å β = 91.500(4)° c = 12.8946(6) Å γ = 92.373(4)°	a = 16.5050(7) Å b = 12.8008(4) Å β = 107.241(4)° c = 11.9517(5) Å
Volume	776.86(6) $Å^3$	2411.66(17) $Å^3$
Z	2	4
Density (calculated)	1.322 Mg/m^3	1.387 Mg/m^3
Absorption coefficient	0.081 mm^{-1}	0.173 mm^{-1}
***F*(000)**	324	1048
Crystal size	0.365 x 0.257 x 0.047 mm^3	0.238 x 0.201 x 0.104 mm^3
θ range for data collection	3.215 to 26.493°	2.959 to 26.496°
Index ranges	$-5 \le h \le 9$, $-11 \le k \le 10$, $-16 \le l \le 14$	$-20 \le h \le 16$, $-16 \le k \le 10$, $-14 \le l \le 14$
Reflections collected	5183	10462
Independent reflections	3200 [R(int) = 0.0129]	4973 [R(int) = 0.0209]
Completeness to θ = 25.242°	99.8 %	99.9 %
Absorption correction	Analytical	Analytical
Max. and min. transmission	0.996 and 0.978	0.985 and 0.969
Refinement method	Full-matrix least-squares on F^2	Full-matrix least-squares on F^2
Data / restraints / parameters	3200 / 0 / 217	4973 / 0 / 338
Goodness-of-fit on F^2	1.008	1.054
Final *R* indices [$I > 2\sigma(I)$]	$R1$ = 0.0436, $wR2$ = 0.1006	$R1$ = 0.0432, $wR2$ = 0.0909
***R* indices (all data)**	$R1$ = 0.0646, $wR2$ = 0.1144	$R1$ = 0.0631, $wR2$ = 0.1001
Largest diff. peak and hole	0.199 and -0.161 $e.Å^{-3}$	0.264 and -0.267 $e.Å^{-3}$

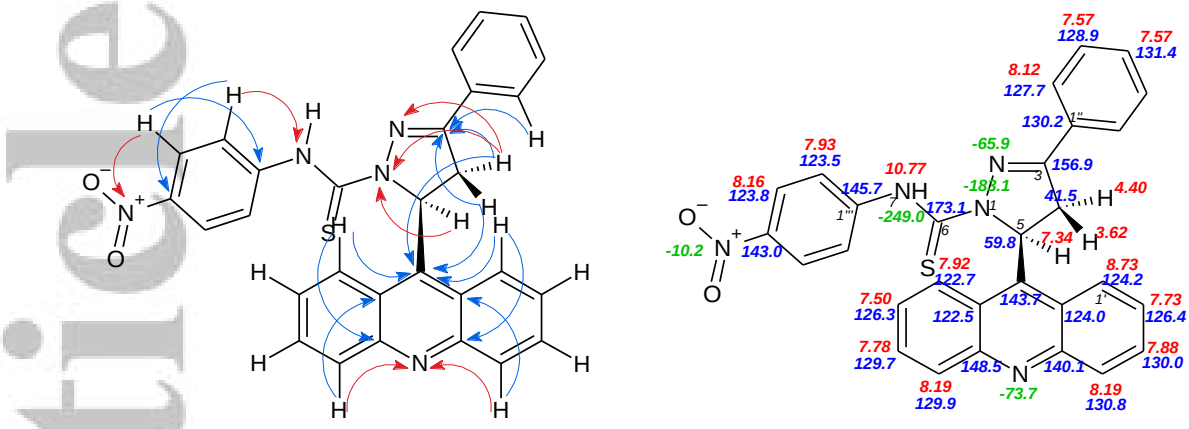

FIGURE 1 Selected $^{1}H,^{13}C$-HMBC (→) and $^{1}H,^{15}N$-HMBC (→) correlations facilitating structural elucidation of **4Ab** (left) and ^{1}H, ^{13}C and ^{15}N chemical shifts (right).

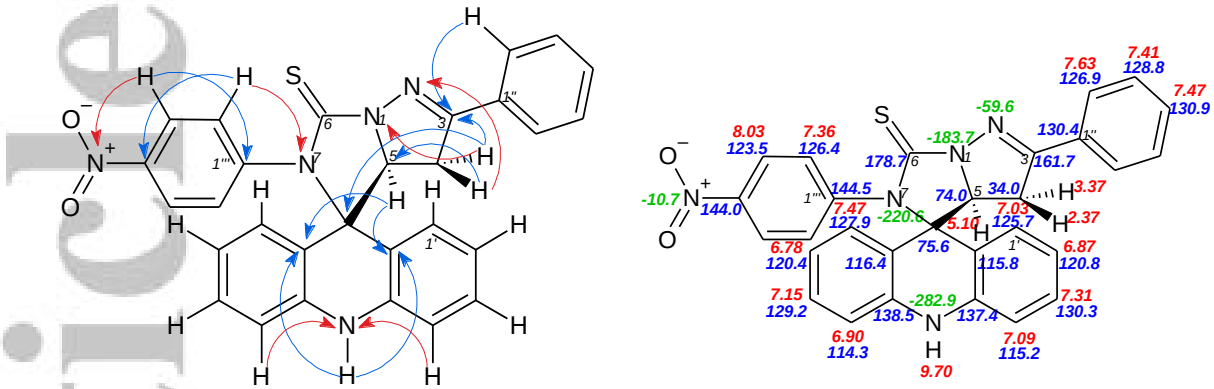

FIGURE 2 Selected $^{1}H,^{13}C$-HMBC (→) and $^{1}H,^{15}N$-HMBC (→) correlations facilitating structural elucidation of **5Ab** (left) and ^{1}H, ^{13}C and ^{15}N chemical shifts (right).

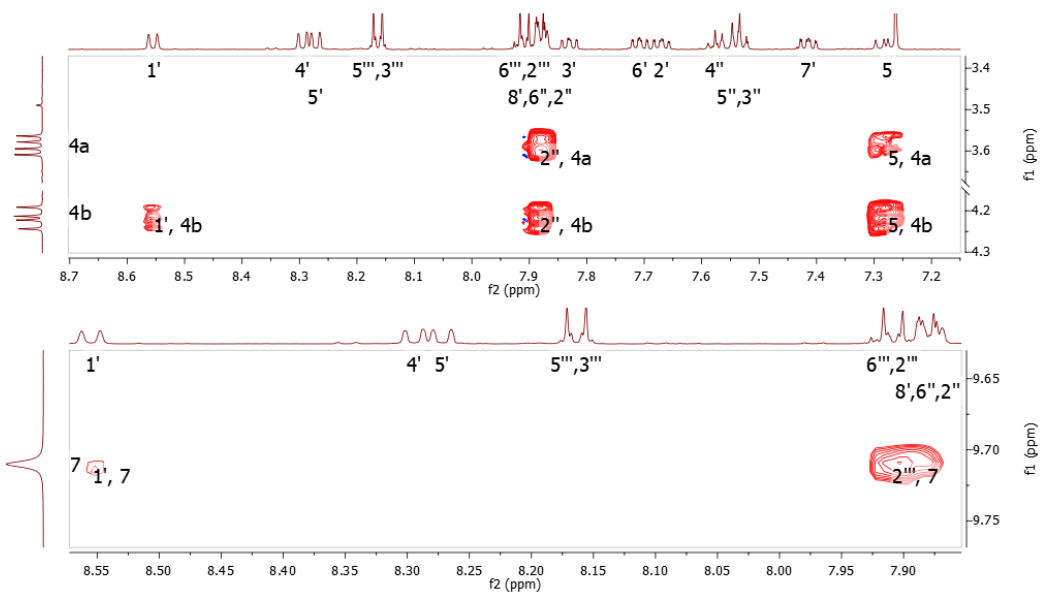

FIGURE 3 2D NOESY spectrum showing key cross peaks for determining relative stereochemistry at C-4 and C-5 of **4Ab** in $CDCl_3$.

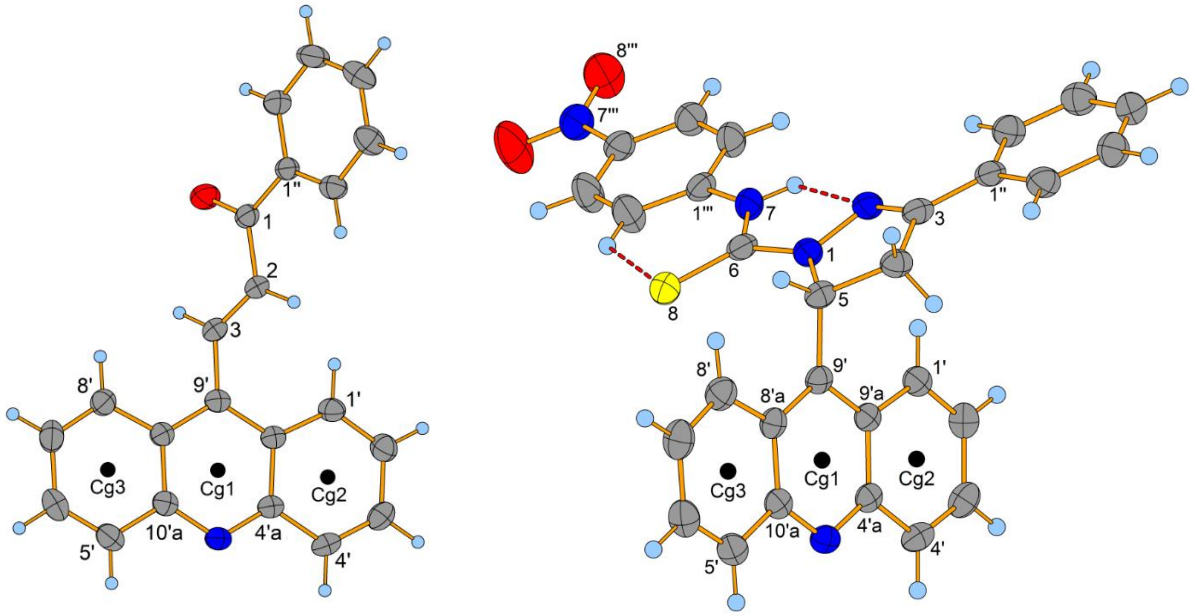

FIGURE 4 Molecular structures of **2A** (left) and **4Ab** (right) with thermal ellipsoids shown at 50% probability. Cg1, Cg2 and Cg3 represent centroids of individual rings of acridine moiety.